

Dynamic behavior of TLP's supporting 5-MW wind turbines under multi-directional waves

Ashraf M. Abou-Rayan^{*}, Nader N. Khalil^a and Mohamed S. Afify^b

*Department of Civil Engineering, Faculty of Engineering Benha, Benha University, Benha Aljadida,
P.O. Box: 13512, Al Qalyubiyah, Egypt*

(Received March 2, 2016, Revised May 2, 2016, Accepted May 7, 2016)

Abstract. Over recent years the offshore wind turbines are becoming more feasible solution to the energy problem, which is crucial for Egypt. In this article a three floating support structure, tension leg platform types (TLP), for 5-MW wind turbine have been considered. The dynamic behavior of a triangular, square, and pentagon TLP configurations under multi-directional regular and random waves have been investigated. The environmental loads have been considered according to the Egyptian Metrological Authority records in northern Red sea zone. The dynamic analysis were carried out using ANSYS-AQWA a finite element analysis software, FAST a wind turbine dynamic software, and MATLAB software. Investigation results give a better understanding of dynamical behavior and stability of the floating wind turbines. Results include time history, Power Spectrum densities (PSD's), and plan stability for all configurations.

Keywords: dynamic response; offshore wind turbines; tension leg platform; wave forces

1. Introduction

Recently, there has been an enormous increase in the global demand for energy as a result of industrial development and population growth, which lead to the current energy crisis. Offshore floating wind farms in shallow or deep waters are the paramount solution for green cost effective renewable energy. The development of related technology in Europe and USA has made a lot of achievement in that field, but in Egypt it is still in its infancy. It is well known that utilizing wind energy at sea is a good solution, since one can achieve better energy efficiency at sea than on land. A rich wind resource lies untapped off the Gulf of Suez coasts of Egypt. This resource is available 8-80 Km. off the Gulf of Suez coast in water depths mostly greater than 30 m. Therefore, the investigation of the dynamic characteristics of wind turbine floating supported structures is very important for Egypt. Differently from fixed structures (Jacket type), floating support structures must provide enough buoyancy to sustain the wind turbine weight. Also, it has to provide enough rotational stability to prevent the system from capsizing and acceptable wave response motions in all its six degrees of freedom to prevent the system from large dynamic loads (Simon and Maurizio

^{*}Corresponding author, Associate Professor, E-mail: Ashraf.aboryan@bhit.bu.edu.eg

^a Assistant Professor, E-mail: Nader.gerges@bhit.bu.edu.eg

^b Graduate Student, E-mail: eng.moh.sami@gmail.com

2012). The following is a brief review of the current research for the wind turbine on floating support structures.

Ramachandran *et al.* (2013), have investigated the response amplitude operators (RAO) for floating offshore wind turbines (spar) using two different codes, FAST and WAMIT (a linear frequency-domain tool). They concluded that the WAMIT can be used as a verification tool for modeling of floating wind turbines in FAST, and that the RAO's for a flexible turbine however cannot be estimated using WAMIT. Takeshi *et al.* (2007), have developed a FEM code to predict the dynamic response of a floating offshore wind turbine system in the time domain, employing the Morison's equation and Nagan *et al.* (2005) model to calculate the hydrodynamic drag forces and inertia forces on the floating structure, and quasi-steady theory to calculate the aerodynamic forces on wind turbines. They found that, the nonlinearity of wave becomes dominant for the water depth less than 100 m and the elastic modes might be resonant with the higher order harmonic component of the nonlinear wave, resulting in the increase of the dynamic response of the floating structure. Zhuangle *et al.* (2013), have developed a finite element model using AQWA to analyze the small-sized floating foundation of a tri-floater and to make a local optimization on the stress concentration area. Ebrahimi *et al.* (2014), have developed a numerical scheme to investigate the dynamic response of a tension leg platform wind turbine (TLPWT) under a parked condition. The obtained data was validated by a scaled-down model fully tested in the marine laboratory. Their results show that the direction of encountering waves is an extremely important factor. Also, wind loads can dampen the oscillation of the model and prevent the impact of large loads on the tethers. Borg *et al.* (2014a, b), have studied the dynamics of a vertical axis wind turbine coupled with three different floating support structures, spar, semi-submersible, and TLP. They have used the FloVAVAT as a design tool with the MATLAB/Simulink environment. Bachynski and Moan (2012), have performed a parametric design on a single-column TLPWT and analyzed it in four different wind-wave conditions. The results indicate that, motions perpendicular to the incoming wind and waves especially in the parked configuration may be critical for TLPWT designs with small displacement. Simon and Maurizio (2012), have investigated a preliminary design of a tri-floater 5-MW wind turbine. The pitch motion has been chosen as the critical design driver for the performance and stability of the support. Lei and Bert (2012), have presented a new method to directly derive the nonlinear equations of motion of a floating wind turbine system using the theorem of conservation of angular momentum and Newton's second law. The results were compared with FAST. Robertson *et al.* (2013), gave a summary for conclusions and recommendations for floating offshore wind systems regarding the limitations of FAST as a modeling tool for offshore wind turbines, as well as the scaled-model testing of these systems. Wang *et al.* (2013), have investigated the potential advantages of floating vertical axis 5-MW wind turbine (FVAWT) mounted on a semisubmersible support structure. They presented the development of a coupled method for modeling of the dynamics of the system considering the wind inflow, aerodynamics, hydrodynamics, structural dynamics and a generator control. Kim and Kim (2016) have numerically simulated the performance of the 5 MW OC4 semisubmersible floating wind turbine in random waves with or without steady/dynamic winds by using the turbine-floater-mooring fully coupled dynamic analysis program FAST-CHARM3D in time domain.

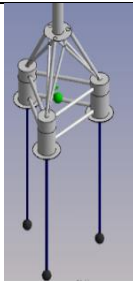
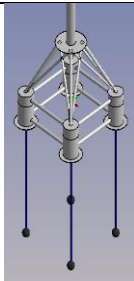
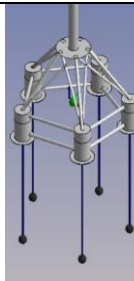
This investigation addresses the dynamic responses of floating offshore wind turbines supported on tension leg platform types. Three floating support structures configurations are considered; the triangular, the square, and the pentagon support configurations. The environmental forces were taken as wind, regular waves, and random waves in multi-directions (0° , 30° , 45° , 90° ,

135⁰, 180⁰), Wind and regular waves properties were taken according to the meteorological data for the red sea (Egyptian Meteorological Authority). Random waves were generated according to Pierson-Moskowitz spectrum (Abou-Rayan, and Hussein 2015). Finite element models were developed for the three configurations using ANSYS-AQWA software (ver.15.0). A 5-MW offshore wind turbine of NREL (National Renewable Energy Laboratory) reference model (Jonkaman *et al.* 2009) was used. The wind turbine effects on the supporting structures were calculated using FAST program (a comprehensive aeroelastic simulator capable of predicting both the extreme and fatigue loads of two- and three-bladed horizontal-axis wind turbines, v.8.0), where the output from FAST were considered as an input for the finite element models. A numerical scheme was written using MATLAB program for computing the PSD's.

2. Descriptions of the TLPWT models

Three configurations were considered in this investigation. Configurations properties and the 5-MW wind turbine property are listed in Tables 1 and 2. Water depth (80 m), columns height, super structure height, side length, and hub height are all kept constant for all three models as shown in Table 2. Also, the total tether stiffness is kept constant.

Table 1 Configurations properties

Properties of the 5-MW wind turbine		Model I	Model II	Model III	
Rotor orientation	Upwind, 3 blades				
Hub diameter	126 m, 3m				
Hub height	90 m				
Max rotor speed	12.1 rpm				
Max tip speed	80 m/s				
Rotor mass	110,000 Kg				
Nacelle mass	240,000 Kg				
Tower mass	347,460 Kg				
Model Shape		Triangle	Square	Pentagon	
Length of the side			40 m		
Floating system	Main column	No.	3	4	5
		Diameter		10 m	
Connecting beam	No.	6	8	10	
	Diameter		2 m		
Super structure	Main beam	No.	3	4	5
		Diameter		2 m	
Bracing	No.	6	8	10	
	Diameter		1.5 m		
Cables	No.	3	4	5	
	Stiffness	2658870 kn/m/ cable			

3. Environmental conditions

The environmental conditions were taken according to the Egyptian Meteorological Authority (EMA) available data for the red sea northern region. Where, the maximum conditions according to the EMA were as following: a) maximum wave height = 4 m, maximum wind speed = 9.0 m/sec. In this investigation the regular wave height, wave period, and constant wind velocity were taken to be 5 m, 12 sec, and 10.0 m/sec, respectively. For the random wave it was taken also as 5 m for wave height and 12 sec. for energy period. It should be noted that, the wind velocity was taken in the direction of the wave. Also, a current load was added as a 10% of the wind load acting linearly in the direction of wind. A regular and random wave forces were considered acting on multi-directions on the three TLPWT configurations with wave heading angles (WHA): 0°, 30°, 45°, 90°, 135°, and 180°, see Fig. 1.

Table 2 Models detailed descriptions

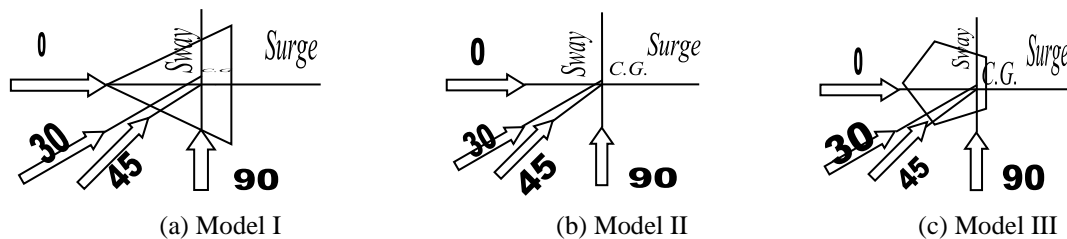
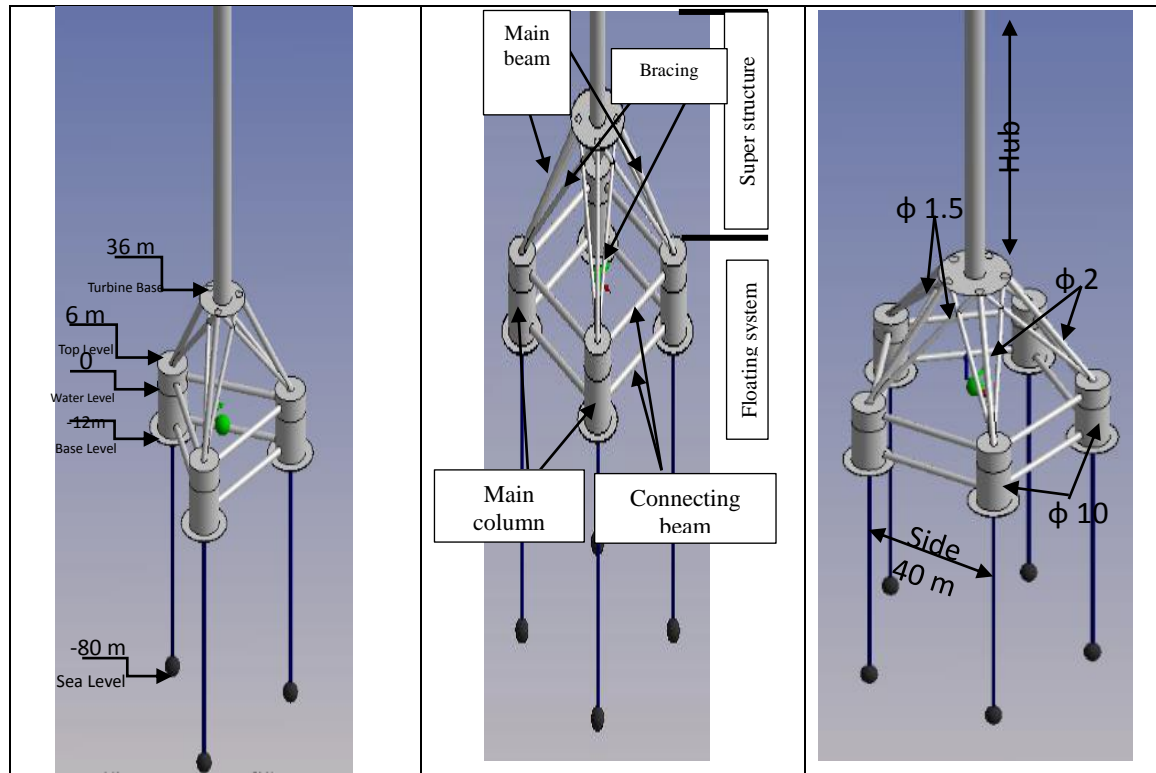


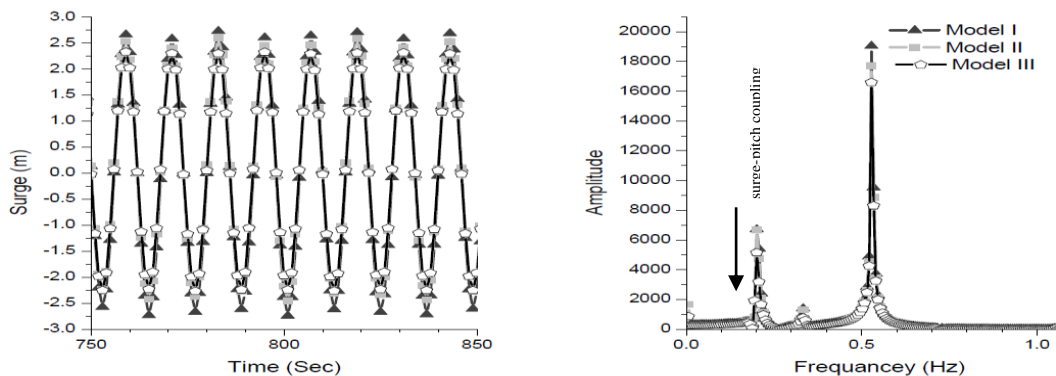
Fig. 1 Multi-directional waves in degrees

4. Results and discussions

FE models with a numerical scheme were developed to obtain the dynamic characteristics for the three models (configurations) mentioned above. Since there are a numerous number of figures, only the essential ones are shown (the response pattern for 180° WHA is the same for 0°, also for 45° WHA has the same pattern as for 135° for all DOF's) . Since heave responses are very small because of cables restrain (heave is a stiff DOF), they are not shown. It should be mentioned that time histories shown are only for a portion of the steady state responses (stationary responses).

4.1 Surge response

Time histories and Power spectrum densities (PSD's) are shown in Figs. 2-5 for all three models of TLPWT's for responses under regular waves. From Figs. 2(a), 3(a), 4(a), and 5(a), it is clear that maximum responses are for the 0° WHA for all models. The highest response among the three models is for the triangular one with ~ 2.64 m., whereas for the square and pentagon configurations were less with about 8% and 17%, respectively, see Fig. 1(a). This is expected because of the geometry differences between models (mass, added mass, and number of pretensioned cables). Also, responses have decrease when the WHA increased (30, 45, and 90 degrees) with about the same response differences as before (8% and 17%). For a 90° WHA (sway direction), responses die out and but it is not zero for all configurations. This is due to the steady state position, so the force excitation is non-zero. For all cases, it is clear from the PSD that the response has a semi-periodic pattern with a period doubling bifurcation (max peak response is at the wave excitation frequency = 0.523 rad/sec.), see Figs. 2(b), 3(b) and 4(b). Moreover, surge-pitch couplings were observed (peaks are clear on the PSD at 0.33 rad/sec, which is the natural frequency for pitch) for the three models with all WHA's except for WHA=90° (This is logic since pitch responses have zero values at this WHA). Furthermore, surge-pitch coupling is inversely proportional to the WHA (surge-pitch coupling is more pronounced with decreasing the wave heading angle). Moreover, it is observed that, increasing the WHA decreases the surge response and giving raise to the sway response to a limit where both are almost equal in amplitude magnitude (case of WHA=45°), which is expected.



(a) Time history

(b) Power spectrum density

Fig. 2 Responses under regular waves, WHA=0°

Time histories response and Power spectrum densities (PSD's) are shown in Figs. 6 and 7 (only 0° and 30° WHA are shown) for all three models of TLPWT's under random waves. All responses have a maximum frequency peak at almost half the excitation frequency. In general, all three models have the same response patterns (i.e., quantitatively) as those due to regular waves. Except that responses in the case of random waves are defiantly chaotic in nature as it is seen from figures. It is obvious the PSD's have multiple frequency responses contributions coming from almost all degrees of freedom.

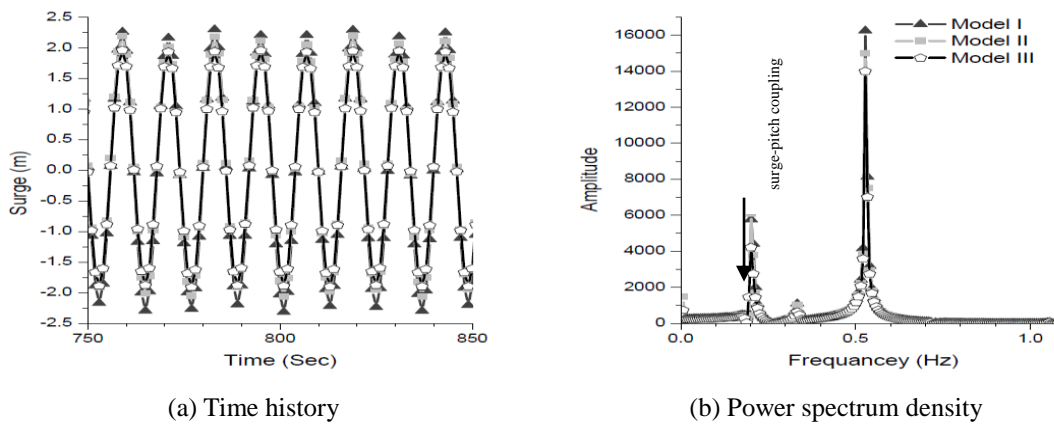


Fig. 3 Responses under regular waves, $WHA=30^\circ$

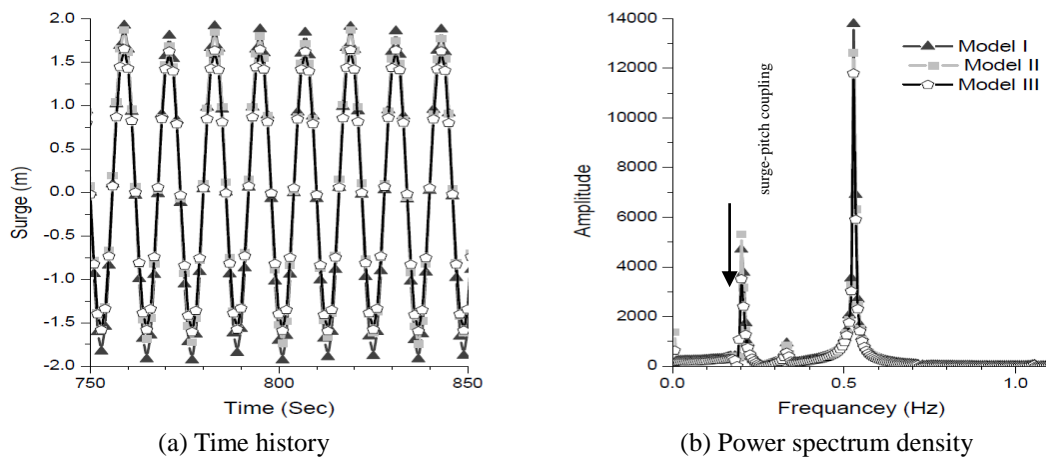


Fig. 4 Responses under regular waves, $WHA=45^\circ$

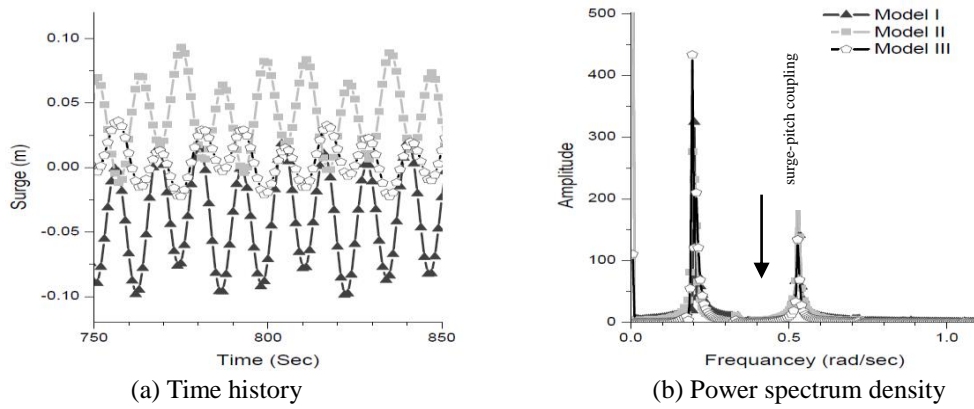


Fig. 5 Responses under regular waves, $WHA=90^0$

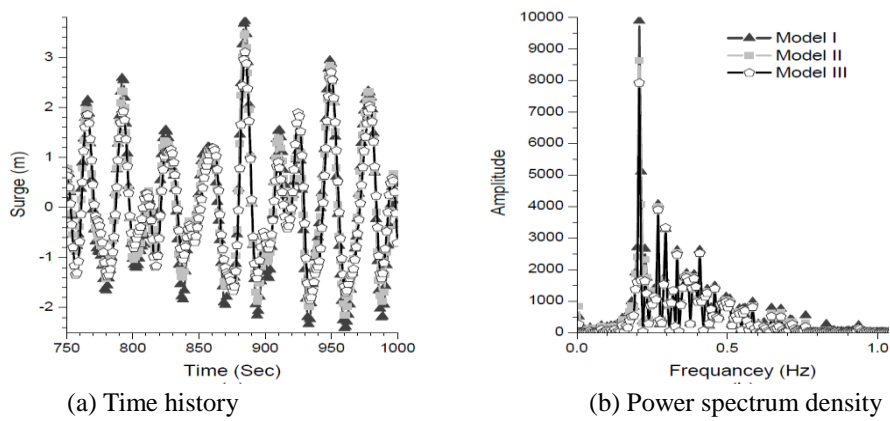


Fig. 6 Responses under random waves, $WHA=0^0$

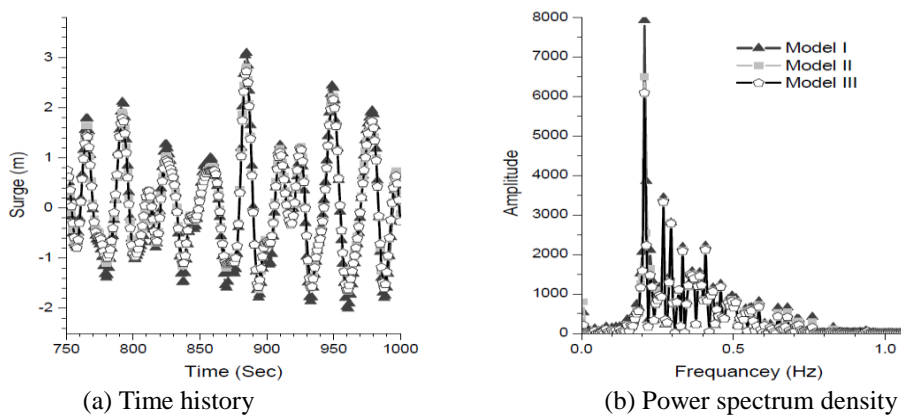


Fig. 7 Responses under random waves, $WHA=30^0$

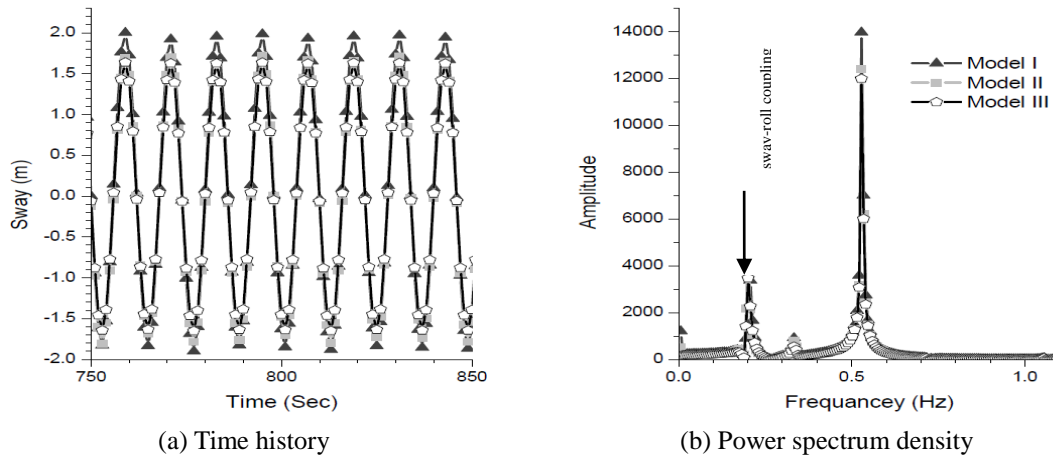


Fig. 8 Responses under regular waves, $WHA=45^\circ$

4.2 Sway response

The same behavior patterns, for regular and random waves, as in the surge response are observed but in a reverse order, see Figs. 8 and 9 (show responses under regular waves only with WHA 45° and 90°). It is noticed that, increasing the WHA activates the response in the sway direction from almost zero to 2.54 m, 2.30 m, and 2.17 m for the triangular, square, and pentagon configurations, respectively (due to regular waves). There are almost 15% increases in the response amplitude due to random waves than those due regular waves, for all configurations. Comparing Figs. 2(a) and 9(a), it is clear that responses for both surge and sway are equal in magnitude and have the same pattern. Also, comparing Figs. 5(a) and 9(a) it is clear that the surge response dies out for the case of $WHA = 90^\circ$ while the sway one reaches its maximum value (contrary to the case of $WHA=0^\circ$). Moreover, a sway-roll couplings (natural frequency for roll = 0.33 rad/sec.) are observed, which is directly proportional to the WHA (only with wave headings 30° , 45° , and 90° for all configurations). For 0° WHA , all configurations, the sway responses die out but after relatively long transition time. Again, responses due to random waves excitations take the same pattern as above but with a chaotic nature as shown in time history and PSD, see fig. 10.

For plan view of surge-sway instability, Fig. 11, it seems like that the pentagon configuration is much more stable in moving on the sea surface, also see Fig. 12. Furthermore, the triangular response under regular waves with $WHA=0^\circ$ is almost triple the pentagon one, although both responses are very small.

4.3 Roll and pitch responses

Roll and pitch responses are affected by the sway and surge responses depending on WHA . Although roll and pitch responses are very small, but an interesting phenomenon can be observed, only in case of regular waves. Responses are modulated, i.e., responses grow over time and then die out for some time and repeat the same pattern again, see Figs. 13, and 14. This is called a modulation response and could be attributed to contributions from other degrees of freedom as shown in the PSD. The modulation

phenomenon was not clearly observed in the case of random waves see Figs. 15 and 16. Moreover, it can be seen from the PSD's Figs. 13(b) and 14(b) that we have a multiple frequencies responses (multiple semi periodic responses) tending to be chaotic under regular waves. For all roll and pitch responses as can be seen from the PSD's there is peak in the almost 1.2 rad/sec. frequency. This could be attributed to contribution from the yaw response, since the yaw natural frequency is 1.2 rad/sec. In the case of random waves, responses are extremely small. Furthermore, PSD's have multi-frequencies contributions coming from all DOF's. Therefore, the motion is obviously chaotic one.

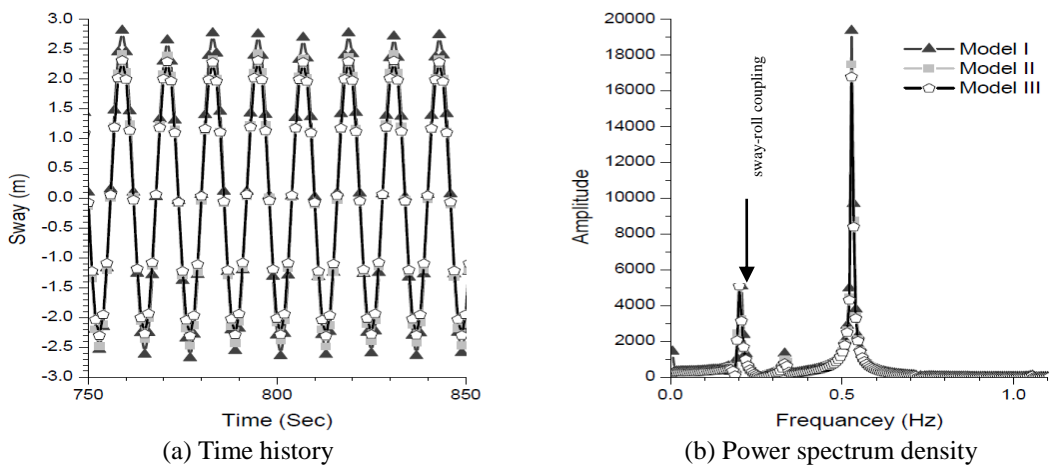


Fig. 9 Responses under regular waves, $WHA=90^0$

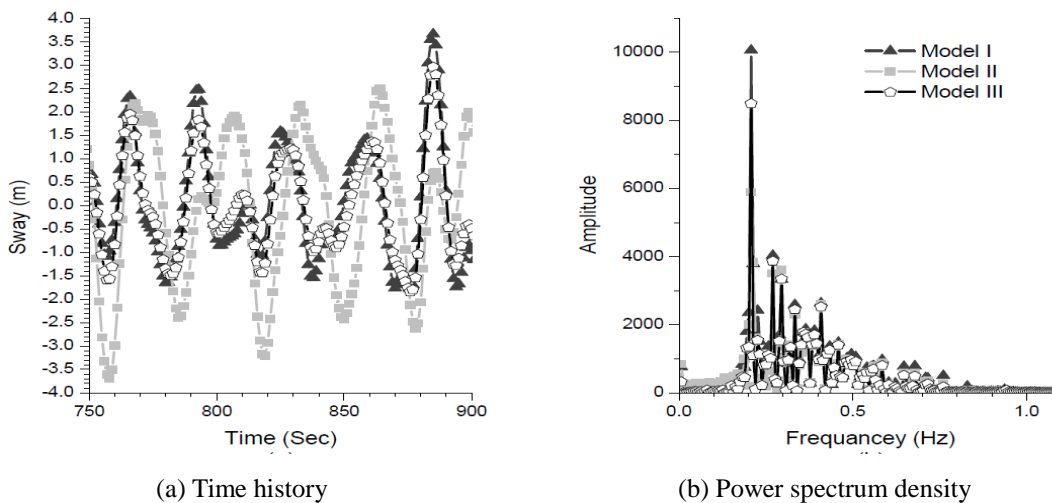


Fig. 10 Responses under random waves, $WHA=90^0$

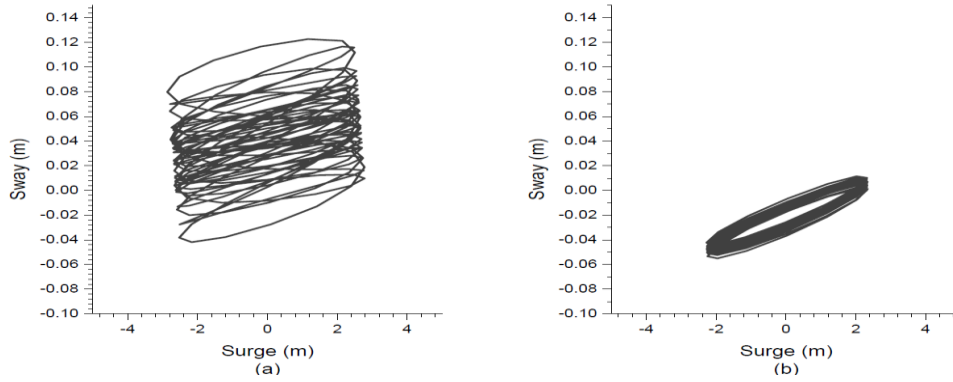


Fig. 11 Instability plane for surge-sway $WHA=0^0$ (a) Model I and (b) Model III

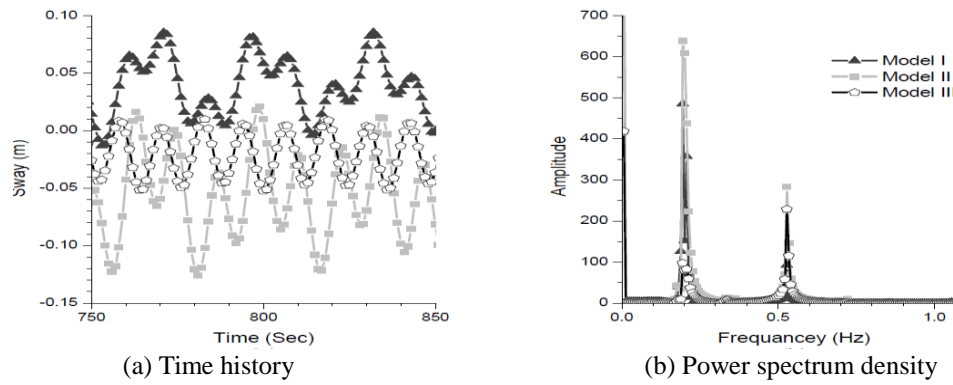


Fig. 12 Responses under regular waves, $WHA=0^0$

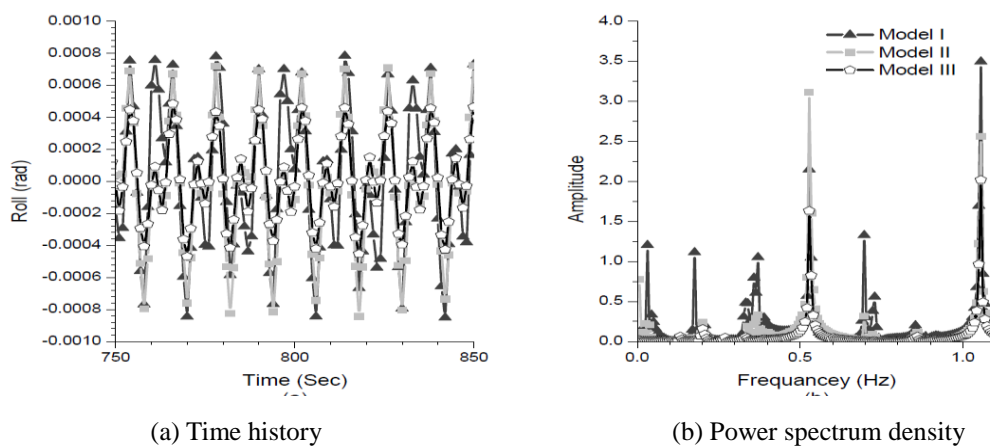


Fig. 13 Responses under regular waves, $WHA=90^0$

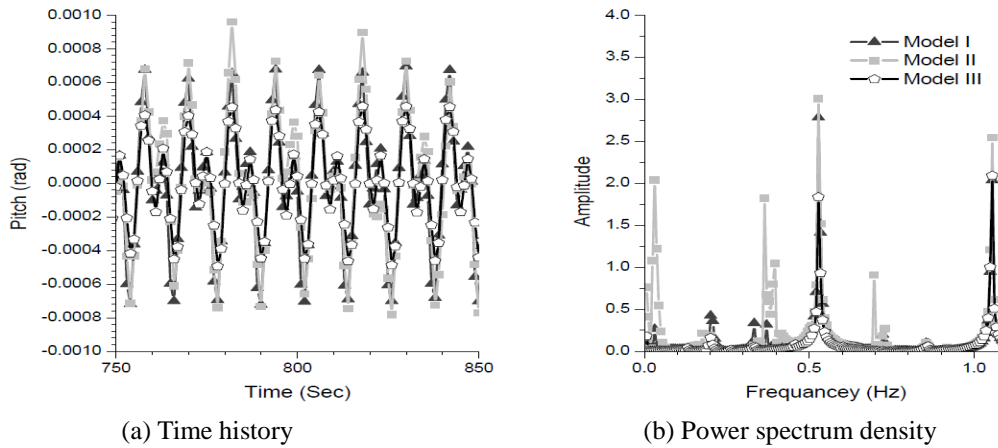


Fig. 14 Responses under regular waves, $WHA=0^{\circ}$ (a) Time history and (b) Power spectrum density

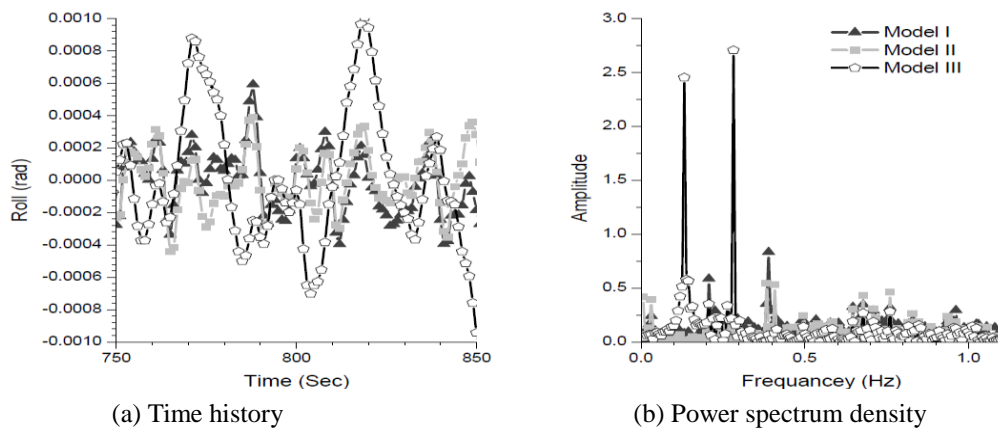


Fig. 15 Responses under random waves, $WHA=90^{\circ}$

4.4 Yaw response

For regular and random wave's excitations, the highest yaw response was found to be about 0.7, 0.5 rad respectively for the case of triangular configuration with WHA of 90° , see Figs. 17, and 18, respectively. This could be attributed to the orientation of the wave to the geometry of the model, see Fig. 1. Again, the pentagon configuration has the lowest response in the yaw DOF for all WHA 's. Also, it was observed that, the yaw response increases as the WHA increases for the triangular configuration. Moreover, it is noticed that the yaw response under regular wave has a period doubling bifurcation, which is not noticed under random wave for $WHA=90^{\circ}$. Furthermore, the same response patterns under regular waves are observed under random waves. In general the maximum yaw responses due to regular or random waves were found in the case of the triangular configuration and the lowest were for pentagon configuration.

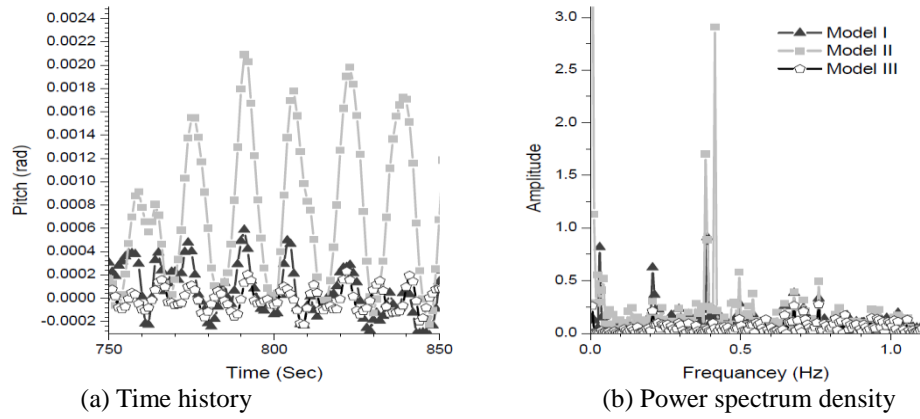


Fig. 16 Responses under random waves, $WHA=0^0$

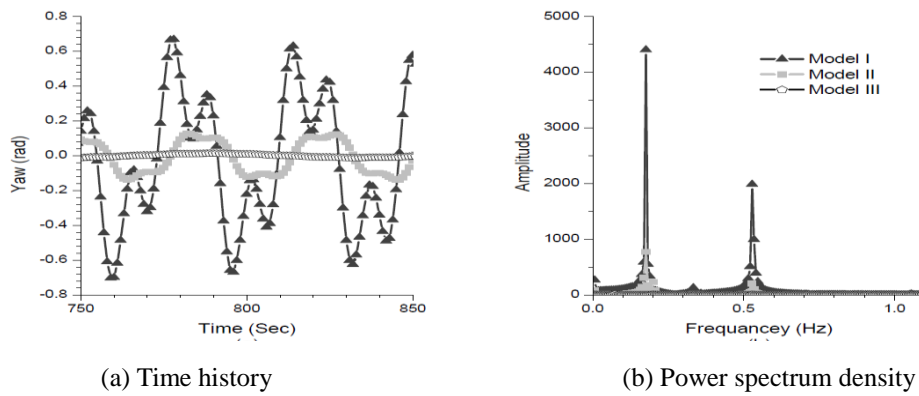


Fig. 17 Responses under regular waves, $WHA=90^0$

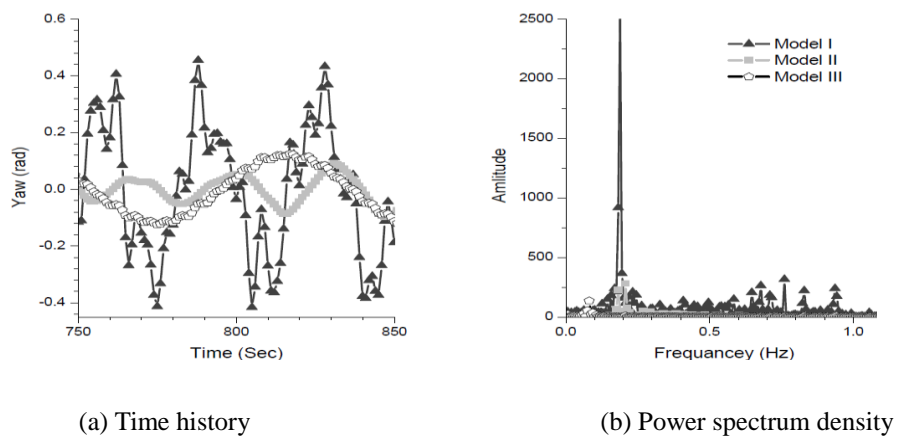


Fig. 18 Responses under random waves, $WHA=90^0$

5. Conclusions

In this paper a proposed pentagon configuration for a TLPWT is proposed and compared with other two configurations, the triangular and square configurations. A finite element models were developed for the three configurations. The NREL 5-MW wind turbine was considered for all configurations. Wave's excitations, regular or random, were considered acting on multi-directions on the three TLPWT configurations. The FAST program by NREL was used to predict the dynamic effect of the 5-MW turbine on the supporting TLP structures. A MATLAB scheme was written to manipulate the data from FAST to the finite element program (ANSYS-AQWA) and to calculate the PSD's.

Based on the aforementioned results and discussions, the following conclusions can be drawn:

- The highest and the lowest responses from all configurations and *WHA*'s were for the triangular and pentagon configurations respectively with 0° *WHA* in the surge direction, wither the waves were regular or random. These responses are expected because of geometry shapes which lead to mass, added mas, and number of pretension cables variances.
- Responses depend significantly on the *WHA*. For the three TLPWT considered, increasing the *WHA* decreasing the surge response and increasing the sway one. In other word, increasing the *WHA* activates specific degrees of freedom which otherwise are not activated under certain *WHA*. This is logically acceptable because of the wave direction.
- The magnitude of motion of the rotational degrees of freedom, roll and pitch depend on the *WHA*, with increasing the *WHA* roll response increases and pitch response decreases. Since, they are very small (in agreement with Koji, 2012) no major change for wind turbine on land to be mounted on TLP's.
- Yaw responses are higher for the triangular configurations than other ones.
- Surge-pitch and sway-roll coupling were observed.
- Responses under regular waves excitations are periodic ones with period doubling bifurcations being observed, for translation degrees of freedom (surge, Sway, and Yaw) and semi-periodic for rotational degree of freedom (roll, pitch, and yaw).
- Responses under random waves excitations are chaotic in nature.

In conclusion the pentagon configuration response is more stable and gives the lowest response compare to the triangular and square configurations but on the other hand it is more costly. Finally it is recommended that an experimental investigation should be considered to compare the numerical results with the experimental ones (this recommendation is in progress).

References

- Abou-Rayam, M.A. and Hussein, S.O. (2015), "Influence of wave approach angle on square tlp's behavior in random sea", *Proceedings of the 2015 world congress, ASEM15*, Incheon, Korea, August.
- Bachynski, E. and Moan, T. (2012), "Design consideration for tension leg platform wind turbines", *Mar. Struct.*, **29**, 89-114.
- Borg, M. and Collu, M. (2014 b), "A comparison on the dynamics of a floating vertical axis wind turbine on three different floating support structures", *Sci. Direct- Energy Procedia*, **52**, 268-279.
- Borg, M., Wang, K., Coullu, M. and Moan, T. (2014a), "Comparison of toe coupled model of dynamics for offshore floating vertical axis wind turbine (VAWT)", *Proceedings of the ASME 33rd international conference on Ocean, Offshore and Arctic Engineering*, San Francisco, USA, June.

- Ebrahimi, A., Abbaspour, M. and Nasiri, R.M. (2014), "Dynamic behavior of a tension leg platform offshore wind turbine under environmental loads", *Scientia Iranica*, **21**(3), 480-491.
- Ishihara, T., Phuc, P.V. and Sukegawa, H. (2007), "A numerical study on the dynamic response of a floating offshore wind turbine system due to resonance and nonlinear wave", *Proceedings of the 2nd EOW*, Berlin, Germany December.
- Jonkman, J., Butterfield, S., Musial, W. and Scott, G. (2009), *Definition of a 5-MW Reference Wind Turbine for Offshore System Development*, National Renewable Energy Laboratory, technical report.
- Kim, H.C. and Kim, M.H. (2016), "Comparison of simulated platform dynamics in steady/dynamic winds and irregular waves for OC4 semi-submersible 5MW wind-turbine against DeepCwind model-test results", *Ocean Syst. Eng.*, **6**(1), 1-21.
- Lefebvre, S. and Collu, M. (2012), "Preliminary design of a floating support structure for 5 MW offshore wind turbine", *Ocean Eng.*, **40**, 15-26.
- Lei, W. and Bert, S. (2012), "Simulation of large-amplitude motion of floating wind turbines using conservation of momentum", *Ocean Eng.*, **42**, 155-164.
- Ramachandran, G.K.V., Robertson, A., Jonkman, J.M. and Masciola M.D. (2013), "Investigation of Response amplitude operators for floating offshore wind turbines", *Proceedings of the 23rd International Ocean, Offshore and Polar Engineering Conference- ISOPE*, Anchorage Alaska. (NREL), June – July.
- Robertson, A., Jonkman, J.M., Musial, W., Vorpahl, F. and Popko, W. (2013), "offshore code comparison collaboration, continuation: Phase II Results of a floating semisubmersible wind system", *Proceedings of the EWEA Offshore*, Frankfurt, Germany, November.
- Srinivasan, N., Chakrabarti, S. and Radha, R. (2005), "Damping-controlled response of a truss-pontoon semi-submersible with heave-plates", *Proceedings of the ASME 2005 24th International Conference on Offshore Mechanics and Arctic Engineering* **1**, June.
- Suzuki, K., Yamaguchi, H., Akasa, M., Imakita, A. and Ishihara, T. (2011), "Initial design of TLP for offshore wind farm", *J. Fluid Sci Technol.*, **6** (3).
- Wang, K., Moan, T. and Hansen, M.O.L. (2013), "A method for modeling of floating vertical axis wind turbine", *Proceedings of the ASME 32nd International conference on ocean, offshore and Arctic Engineering*, Nantes, France, June.
- Yao, Z.L., Chen, C.H. and Chen, Y.M. (2013), "Research on the dynamic response of floating foundation of a tri-floater offshore wind turbine", *Appl. Mech. Mater.*, **257**, 852-855.